Available online at www.eccomasproceedia.org
Eccomas Proceedia COMPDYN (2017) 5035-5044

ECCOMAS
Proceedia

COMPDYN 2017
6th ECCOMAS Thematic Conference on
Computational Methods in Structural Dynamics and Earthquake Engineering
M. Papadrakakis, M. Fragiadakis (eds.)
Rhodes Island, Greece, 15–17 June 2017

MODELING FLEXURE-SHEAR FAILURES IN MASONRY-INFILLED RC FRAMES WITH INELASTIC FIBER-BASED FRAME ELEMENTS

Alexander Kagermanov[1], **Paola Ceresa**[2]

[1] UME School, Institute for Advanced Studies (IUSS)
Piazza della Vittoria, 15, 27100, Pavia, Italy
alexander.kagermanov@umeschool.it

[2] Institute for Advanced Studies (IUSS)
Piazza della Vittoria, 15, 27100, Pavia, Italy
paola.ceresa@iusspavia.it

Keywords: inelastic frame elements, shear failure, flexure-shear interaction, masonry infills.

Abstract. *A numerical procedure for modeling beam and/or column shear failures in RC infilled frames is presented. The main novelty relies in the use of inelastic fiber-based frame elements with flexure-shear interaction for modeling the RC members. The frame element is based on the Timoshenko beam kinematic assumption combined with an orthotropic smeared-crack constitutive model for cracked concrete, which is defined at each section fiber for the determination of the nonlinear sectional response. For the masonry panel, the equivalent multiple-strut approach is adopted, in order to accurately predict the distribution of shear and bending moments in the RC members due to infill-frame interaction. The procedure is verified against available monotonic tests where flexure-shear failures of the RC members were observed during the test. Comparison with traditional flexural frame elements is also provided in order to highlight the differences between the two methodologies.*

Peer-review under responsibility of the organizing committee of COMPDYN 2017.
doi: 10.7712/120117.5782.17526

1 INTRODUCTION

The seismic behavior of masonry-infilled RC frames has been object of extensive experimental and analytical research mainly for two reasons: (i) its widespread use in many seismic regions, such as Mediterranean countries and South America, and (ii) the complex interaction between the frame and infill panel, which can negatively affect the failure mode and overall ductility of the structure. Typically, five basic failure modes have been identified from field and experimental investigations [1, 2, 3, 4, 5, 6]: (i) Sliding shear along horizontal bed joints, (ii) diagonal tension failure, (iii) diagonal compression failure, (iv) corner crushing of the panel and (v) flexure or shear-flexure failure of the RC members. Among them, failure of the columns directly compromises the vertical load carrying capacity of the structure. In particular, flexure-shear failure can significantly reduce the overall ductility due to its brittle nature, especially in the case of weak frame-weak masonry system.

At the same time, modeling of masonry-infilled frames for nonlinear static and dynamic analysis has been typically approached with macro-models consisting in a pair of equivalent diagonal struts, one in each direction, with a predefined hysteretic response. Although this approach may provide credible results in terms of overall strength and stiffness, upon appropriate selection of the strut parameters, it is not able to simulate the correct location and type of failure in the RC members, since it does not adequately reproduce the distribution of bending moments and shear forces [6, 7]. Hence, a more appropriate approach is to use multiple-strut models such as those introduced in [8, 9].

An important shortcoming in simulating failure mode (v) using frame analysis is the inability of flexural frame elements in capturing shear failures. Although this problem can be partially solved with equivalent lumped plasticity models with flexure-shear hinges [10], this approach requires the calibration of several model parameters, which is rather complicated in the case of masonry-infilled RC frames due to the scarcity of the available experimental data. Hence, an alternative approach is pursued herein based on fiber frame elements combined with biaxial constitutive models for reinforced concrete, which provides a more rational way of modeling flexure-shear interaction in RC members.

A case-study masonry infilled RC frame, which experienced shear failure of the columns, was selected from the literature [11, 12]. The frame was modeled with both traditional flexural frame elements and those with flexure-shear interaction. A three-strut approach was used to represent the masonry panel in order to capture more accurately the shear and flexural demands in beams and columns. Finally, comparison in terms of lateral-force displacement response is provided in order to highlight the differences between the two modeling approaches**.**

2 FRAME ELEMENT WITH AXIAL-SHEAR INTERACTION

The inelastic frame element used in the present work is based on the Timoshenko beam theory at the kinematic level, combined with biaxial constitutive models for reinforced concrete at the fiber section level. Several element formulations have been previously presented following a similar approach [13, 14, 15]. The main differences, however, concerned the type of constitutive model for reinforced concrete, e.g. damage-plasticity, orthotropic, micro-plane models, etc…, the type of element formulation, e.g. displacement-based, force-based or mixed formulation, and the type of shear strain profile over the cross section, e.g. uniform, parabolic or exact. Despite the different modeling approaches, overall acceptable performance has been demonstrated by the different authors.

In what follows, a brief summary of the element formulation used herein is presented. Further details can be found in [16].

The total displacement (u, v) at a given point of the section with coordinates (x, y) is given assuming the plane section assumption (Figure 1):

$$u(x,y) = u_o(x) - \theta_z(x)y \tag{1}$$

$$v(x,y) = v_o(x) \tag{2}$$

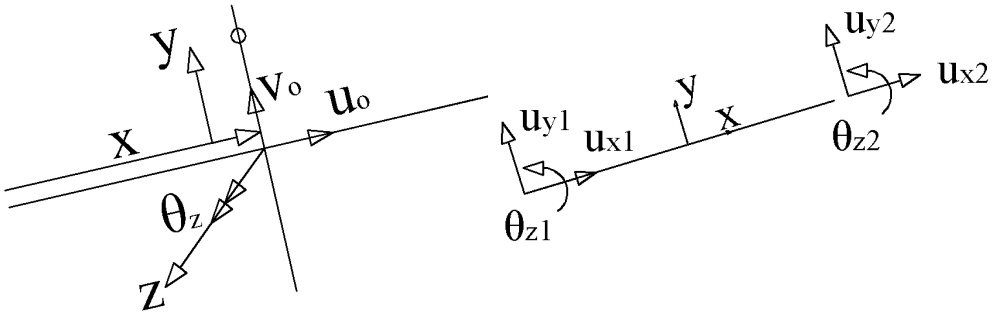

Figure 1: Definition of frame element reference system and kinematics.

where u_o is the horizontal displacement, θ_z the section rotation and v_o the vertical displacement of the beam axis, x the longitudinal coordinate along the beam axis, and y the vertical coordinate. Assuming small strain-displacement compatibility, axial and shear strains at each fiber are given as:

$$\begin{pmatrix} \varepsilon_x \\ \gamma_{xy} \end{pmatrix} = \begin{bmatrix} 1 & -y & 0 \\ 0 & 0 & 1 \end{bmatrix} \begin{pmatrix} \varepsilon_o \\ \chi_z \\ \gamma_{oy} \end{pmatrix} \tag{3}$$

$$\boldsymbol{\varepsilon} = \mathbf{B}\mathbf{e} \tag{4}$$

where ε_x and γ_{xy} are the axial and shear strains, respectively, acting on a section layer of coordinate y, ε_o is the average axial strain, χ_z the section curvature and γ_{oy} the section shear deformation. Section forces are obtained from direct integration of stress distributions over the section:

$$\mathbf{S} = \int_A \mathbf{B}^T \boldsymbol{\sigma} dA \tag{5}$$

where $\mathbf{S}=[N, M, V]^T$ and $\boldsymbol{\sigma}=[\sigma_x, \tau_{xy}]^T$ are the vector of section forces and stresses, respectively. The tangent stiffness matrix of the section is obtained taking variation of section forces with respect to section deformations:

$$\mathbf{K}_s = \frac{\partial \mathbf{S}}{\partial \mathbf{e}} = \frac{\partial}{\partial \mathbf{e}} \int_A \mathbf{B}^T \boldsymbol{\sigma} dA = \int_A \mathbf{B}^T \frac{\partial \boldsymbol{\sigma}}{\partial \boldsymbol{\varepsilon}} \frac{\partial \boldsymbol{\varepsilon}}{\partial \mathbf{e}} dA = \int_A \mathbf{B}^T \frac{\partial \boldsymbol{\sigma}}{\partial \boldsymbol{\varepsilon}} \mathbf{B} dA = \int_A \mathbf{B}^T \bar{\mathbf{D}} \mathbf{B} dA \tag{6}$$

where $\bar{\mathbf{D}}$ is the 2×2 material stiffness matrix, obtained from an orthotropic, smeared-crack constitutive model presented in [17], upon imposing $\sigma_y=0$ at each section layer.

The element formulation presented so far was implemented in a displacement-based Timoshenko beam element, using linear interpolation functions for u_o, v_o and θ_z. Reduced integration was used in order to avoid shear locking, with one Gauss integration point per element. At the sectional level, a parabolic shear strain profile was adopted as a function of γ_{oy}:

$$\gamma_{xy} = \frac{3}{2}\gamma_{oy}(1-(2y/h)^2) \tag{7}$$

where h is the section height.

3 MODELING THE INFILL PANEL

The infil panel was modeled using three equivalent struts connected between the corners of the frame as depicted in Figure 2. Different models are available in the literature to estimate the properties of the struts [8, 9, 18, 19]. However, since in the present context the main objective is to assess the performance of inelastic frame elements with flexure-shear interaction, these properties were calibrated such as to fit the experimental data.

The axial force-displacement behavior of each strut is described by the Popovics envelope (Figure 2), given as:

$$F = \frac{F_m x r}{r - 1 + x^r} \tag{8}$$

$$r = \frac{E_{tg}}{E_{tg} - E_{sec}} \tag{9}$$

where F_m is the peak force, x is the ratio between the axial displacement to the peak displacement δ/δ_m, and E_{tg} and E_{sec} are the tangent and secant (to the peak) moduli respectively. The same type of envelope is assumed for the three struts. However, based on tributary areas, the strength of the off-diagonal struts is taken as 50% that of the central strut. In this way only three parameters need to be calibrated for the entire panel: F_m, δ_m and E_{tg}.

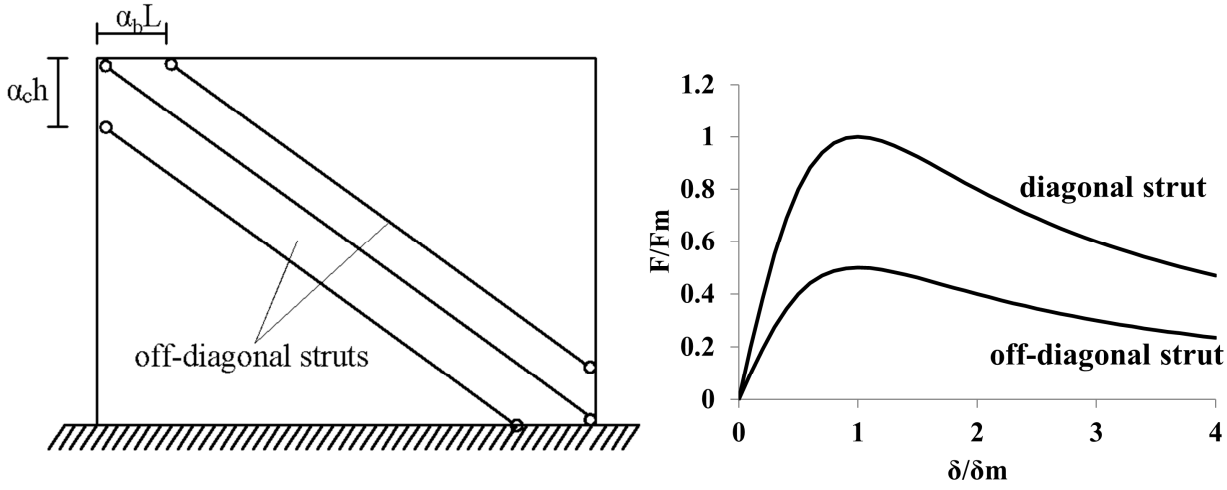

Figure 2: Multiple-strut representation of infill panel and monotonic envelopes of the diagonal struts.

Another important parameter is the location of the off-diagonal strut, represented by the parameters α_c and α_b (Figure 2), which is associated to the position of the plastic hinge in the beam or column, respectively. Theoretical values for this parameter were given by Liauw and Kwan (1983) [20, 21] for different collapse mechanisms, which will be used in the next section.

4 CASE STUDY

The selected case study frame, shown in Figure 3, was part of a large experimental campaign carried out by Mehrabi and Shing [11, 12]. The specimen consisted of a ½-scale, one-story one-bay prototype designed as a weak frame for lateral wind only (1.24kPa), without consideration of the masonry infill. For the infill, 0.1×0.1×0.2 m solid masonry blocks with 9.5mm thick mortar bed joints were used. Material properties for concrete, reinforcement and masonry panel are summarized in Table 1 and Table 2. The specimen was subjected to an increasing lateral force applied at the top beam, and two vertical loads (146.8kN each) concentrated at the top of the columns.

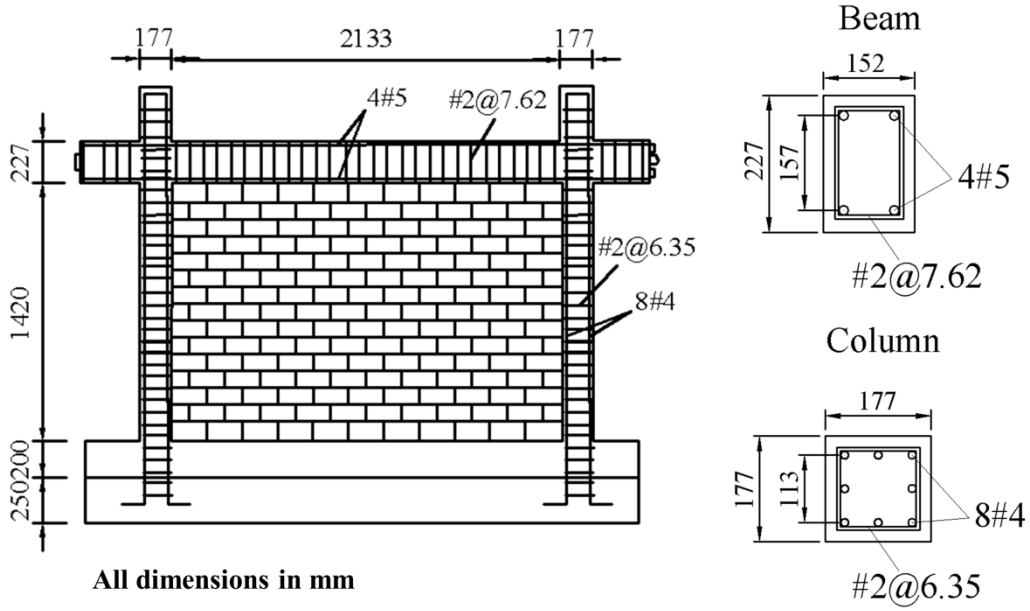

Figure 3: RC masonry-infilled frame: geometry and cross-sections (adapted from [11]).

	Concrete			Masonry prisms		Masonry Units	Mortar
Frame	f_c(MPa)	ε_o	f_t(MPa)	$f_{m\text{-}90}$ (MPa)	$\varepsilon_{m\text{-}90}$	f_{mu}(MPa)	f_{mr}(MPa)
Bare	30.8	0.0018	3.24	-	-		
Infilled	30.8	0.0018	3.24	15.1	0.0029	15.6	15.9

f_c, ε_o*: compressive strength and strain at peak stress of concrete;* f_t*: tensile strength of concrete;* $f_{m\text{-}90}$, $\varepsilon_{m\text{-}90}$*: compressive strength and strain at peak stress perpendicular to the bed joints;* f_{mu}*: compressive strength of masonry units;* f_{mr}*: compressive strength of mortar*

Table 1: Material properties for concrete and masonry.

Bar size	Type	Nominal diameter (mm)	Yield stress (MPa)	Ultimate stress (MPa)
#2	Plain	6.35	367	449
#4	Deformed	12.7	420	661
#5	Deformed	15.8	413	661

Table 2: Material properties for steel.

The finite element model of the frame is shown in Figure 4. The frame elements were defined along the centerline of the members, with an element extending into the base beam 200mm, referred to as joint element, in order to consider the joint flexibility and strain penetration effects. This element had the same properties as the rest of the column elements, but with a reinforcement ratio 3 times that of the columns. The masonry struts were connected between the locations of plastic hinge regions, defined hereafter, such as to simulate a short-column effect.

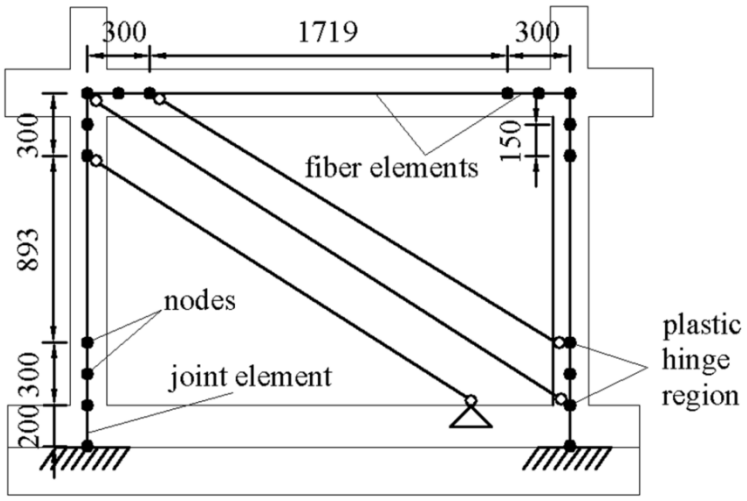

Figure 4: Finite element model of the inflll frame.

The location of the plastic hinges in the columns was determined from plastic limit analysis as [20, 21]:

$$\alpha_c = \sqrt{\frac{2(M_c + M_j)}{\sigma_c t h^2}} \tag{10}$$

where M_c is the column flexural strength, M_j is the joint flexural strength taken as min(M_c, M_b), M_b being the beam flexural strength. t is the panel thickness, and h the story height. σ_c is the crushing stress of the panel material, which can be estimated as [22]:

$$\sigma_c = \frac{f_{m-0}}{\sqrt{1 + 3\mu^2 r^4}} \tag{11}$$

where μ is the friction coefficient between the panel and the RC frame, r is the panel aspect ratio, and f_{m-0} is the masonry strength parallel to the bed joints. It can be assumed that $\mu \approx 0$ due to concrete shrinkage, hence $\sigma_c = f_{m-0}$. f_{m-0} has been related to the masonry strength perpendicular to the bed joints, f_{m-90}, given in Table.1 as $f_{m-0}=0.70 f_{m-90}$ [23].

Upon substitution in Equation 10, with $M_c=M_j=20.9$kNm, $\sigma_c=10.8$ MPa, t=0.0921m and h=1.634m, a value of 0.18 is obtained for α_c. The same value is assumed for the beams, α_b. Thus, the location of the plastic hinge is approximately 0.30m from the beam-column joint. Two elements were defined in this region, 150mm each, as shown in Figure 4.

Comparison between experimental and numerical lateral force-displacement response, for both bare and infill frames, is shown in Figure 5. Results from the traditional flexural (Euler-Bernouilli) beam element, based on uniaxial constitutive laws, have been included as well.

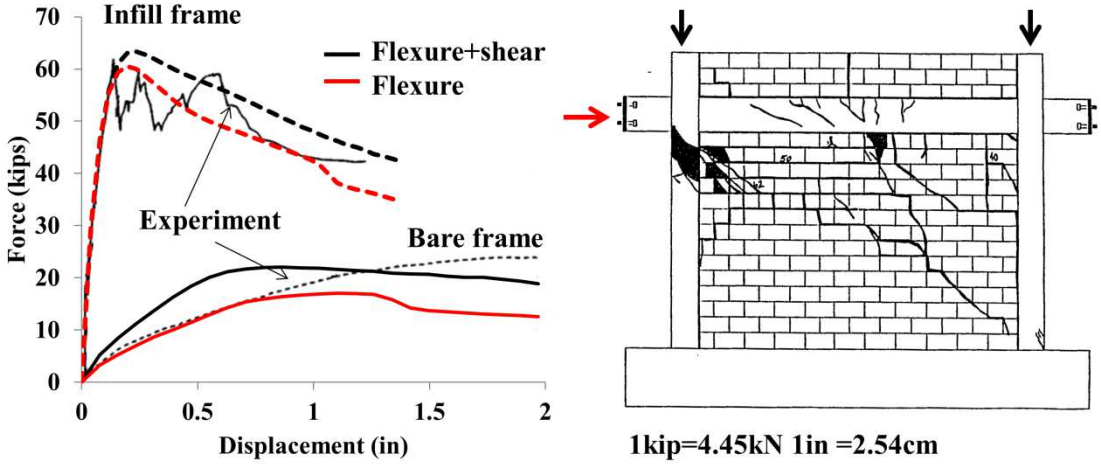

Figure 5: Lateral force-displacement response and observed experimental damage [11].

The bare frame response is predominantly in flexure, ultimately failing upon concrete crushing at the bottom of the leeward column. In the experiment, the damage pattern for the infilled frame involved diagonal tension failure of the panel and flexure-shear failure at the top windward column (Figure 5).

For the bare frame, it is noted that the flexure-shear element is stiffer and stronger since shear resisting mechanisms are included in addition to the flexural ones, and no shear failure occurs. For the infilled frame, it seems that flexure-shear interaction has a minor influence on the overall response, which is governed by the masonry struts.

The latter is also demonstrated from the distribution of bending moment and shear demands at the maximum lateral load (Figure 6), from where it can be seen that for both elements the distribution is very similar, and highly concentrated in the short-column and short-beam portions.

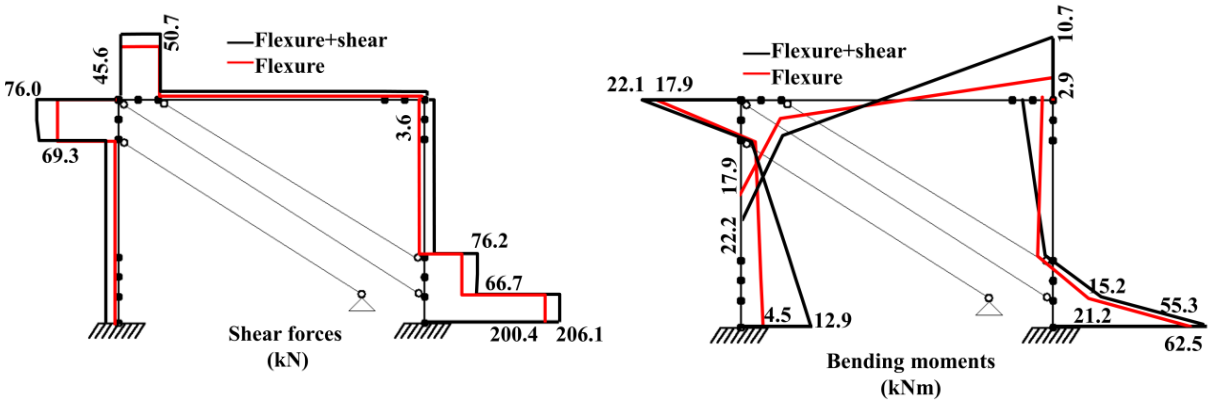

Figure 6: Bending moment and shear distributions

Despite being the global response similar for both types of elements, the internal resisting mechanisms are clearly different. As an example, strains in the transverse reinforcement obtained from the flexure-shear element at different levels of lateral displacement are shown below (Figure 7). These correspond to the Gauss integration point in the top element of the windward column. It is noted that yielding does not occur at the maximum lateral load (0.24in), but it does occur in subsequent load steps when the masonry struts enter the post-peak softening branch.

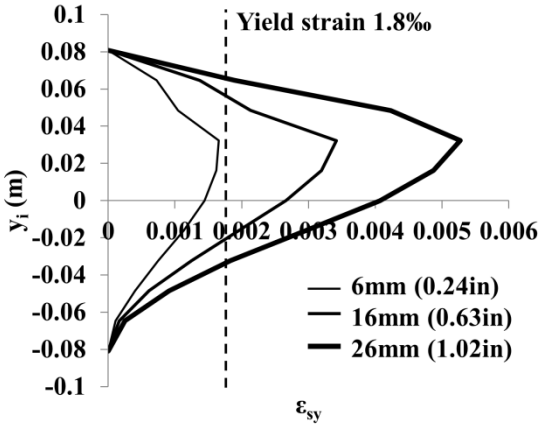

Figure 7: Strains in the transverse reinforcement at different displacement levels.

5 CONCLUSIONS

Preliminary results presented here on the evaluation of flexure-shear fiber-based frame elements for modeling RC infilled frames demonstrated that similar global results are obtained when compared to the traditional flexural element, at least in terms of lateral force-displacement response, and bending and shear force distributions. However, these conclusions are based on a single case study which involved a weak frame-strong masonry RC frame, whereby the infill panel significantly contributed to both lateral and vertical stiffness and strength. Although multiple peaks were experimentally observed in the post-peak response of the infilled frame, possibly due to cracking and sliding of the panel, stress redistribution between the frame and the panel, and flexure-shear failure of the columns, the numerical model did not show this behavior.

Notwithstanding, some local results from the flexure-shear element, such as strains in the transverse reinforcement, indicated that substantial demands were imposed in the short-column region, where shear failure was observed during the experiment. Yielding of transverse reinforcement was attained in the post-peak range of the infilled frame.

It is recommended to carry out further validation, particularly for weak frame-weak masonry structures, where the limitations of brittle shear failure on global ductility capacity can be better quantified.

REFERENCES

[1] M. N. Fardis, and G. M. Calvi, Effects of infills on the global response of reinforced concrete frames. *Proc., 10th European Conf. on Earthquake Engineering, European Association for Earthquake Engineering (EAEE)*, Istanbul, Turkey, 2331–2336, 1994.

[2] B. Stafford Smith, Behavior of square infilled frames. *J. Struct. Div.*, **92**(1), 381–403, 1966.

[3] L. D. Decanini, and G. E. Fantin, Modelos simplificados de la mampostería incluida en porticos. Características de rigidez y resistencia lateral en astado límite. *Jornadas Argentinas de Ingeniería Estructural III, Vol. 2, Asociacion de Ingenieros Estructurales*, Buenos Aires, Argentina, 817–836, 1987 (in Spanish).

[4] H. Rodrigues, H. Varum, and A. Costa, A non-linear masonry infill macro-model to represent the global behaviour of buildings under cyclic loading. *Int. J. Mech. Mat. Des*., **4**(2), 123–135, 2008.

[5] T. Paulay, and M. J. N. Pristley, *Seismic design of reinforced concrete and masonry buildings*, Wiley, New York, 744, 1992.

[6] F. J. Crisafulli, A. J. Carr, and R. Park, Analytical modelling of infilled frame structures—A general review. *Bull. New Zealand Soc. Earthquake Eng.*, **33**(1), 30–47, 2000.

[7] J. Reflak, and P. Fajfar, Elastic analysis of infilled frames using substructures. *Proc., 6th Canadian Conf. on Earthquake Engineering*, University of Toronto Press, Toronto, 285–292, 1991.

[8] V. Thiruvengadam, On the natural frequencies of infilled frames. *Earthquake Eng. Struct. Dyn.*, **13**(3), 401–419, 1985.

[9] C. Z. Chrysostomou, P. Gergely, and J. F. Abel, A six-strut model for nonlinear dynamic analysis of steel infilled frames. *Int. J. Struct. Stab. Dyn.*, **2**(3), 335–353, 2002.

[10] P. E. Mergos, A. J. Kappos, A distributed shear and flexural flexibility model with shear–flexure interaction for R/C members subjected to seismic loading. *Earthquake Engineering & Structural Dynamics*, **37**(12), 1349–1370, 2008.

[11] A. B. Mehrabi, and P. B. Shing, Finite element modeling of masonry-infilled RC frames. *J. Struct. Eng.*, **123**(5), 604–613, 1997.

[12] A. B. Mehrabi, P. B. Shing, M. Schuller, and J. Noland, Experimental evaluation of masonry-infilled RC frames. *J. Struct. Eng.*, **122**(3), 228–237, 1996.

[13] P. Ceresa, L. Petrini, R. Pinho, R. Sousa, A fibre flexure–shear model for seismic analysis of RC-framed structures, *Earthquake Engineering and Structural Dynamics*, **38**, 565-586, 2009.

[14] M. Petrangeli, P. E. Pinto, V. Ciampi, Fibre element for cyclic bending and shear of RC structures. I: theory, *Journal of Engineering Mechanics*, **125**(9), 994-1001, 1999.

[15] S. Guner, and F. J. Vecchio, Analysis of Shear-Critical Reinforced Concrete Plane Frame Elements under Cyclic Loading, *Journal of Structural Engineering (ASCE)*, **137** (8), pp. 834-843, 2011.

[16] A. Kagermanov, P. Ceresa, An exact shear strain approach for rc frame elements with axial-shear interaction, *VII European Congress on Computational Methods in Applied , Sciences and Engineering (ECCOMA)*, M. Papadrakakis, V. Papadopoulos, G. Stefanou, V. Plevris, Crete Island, Greece, 5–10, June 2016

[17] A. Kagermanov, P. Ceresa, Physically-based cyclic tensile model for reinforced concrete membrane elements, *Journal of Structural Engineering (ASCE),* **142**(12), December, 2016

[18] R. O. Hamburger, and A. S. Chakradeo, Methodology for seismic-capacity evaluation of steel-frame buildings with infill unreinforced masonry. *Proc., National Earthquake Conf.*, Vol. 2, Central U.S. Earthquake Consortium, Memphis, TN, 173–191, 1993.

[19] W. W. El-Dakhakhni, M. Elgaaly, and A. A. Hamid, Three-strut model for concrete masonry-infilled frames. *J. Struct. Eng.*, **129**(2), 177–185, 2003.

[20] T. C. Liauw, and K. H. Kwan, Plastic theory of infilled frames with finite interface shear strength. *ICE Proc.*, **75**(4), 707–723, 1983.

[21] T. C. Liauw, and K. H. Kwan, Plastic theory of non-integral infilled frames. *ICE Proc.*, **75**(3), 379–396, 1983b.

[22] A. Saneinejad, B. Hobbs, Inelastic design of infilled frames, *J. Struct. Eng. (ASCE)*, **121**(4), 634-650, 1995.

[23] C.K. Seah, Universal approach for the analysis and design of infilled frame structures, PhD Thesis, Univ. of New Brunswick, Fredericton, Canada, 1995.